THE JOURNAL OF BIOLOGICAL CHEMISTRY VOL. 291, NO. 8, pp. 4236–4246, February 19, 2016

Filamin A Is Involved in HIV-1 Vpu-mediated Evasion of Host Restriction by Modulating Tetherin Expression*

Received for publication, December 2, 2015, and in revised form, January 6, 2016 Published, JBC Papers in Press, January 7, 2016, DOI 10.1074/jbc.M115.708123

Dominique Dotson[‡§], Elvin A. Woodruff[‡§], Fernando Villalta[‡§], and Xinhong Dong[‡§1]

From the [‡]Department of Microbiology and Immunology and [§]Center for AIDS Health Disparities Research, School of Medicine, Meharry Medical College, Nashville, Tennessee 37208

Tetherin, also known as bone marrow stromal antigen 2 (BST-2), inhibits the release of a wide range of enveloped viruses, including human immunodeficiency virus, type 1 (HIV-1) by directly tethering nascent virions to the surface of infected cells. The HIV-1 accessary protein Vpu counteracts tetherin restriction via sequestration, down-regulation, and/or displacement mechanisms to remove tetherin from sites of virus budding. However, the exact mechanism of Vpu-mediated antagonism of tetherin restriction remains to be fully understood. Here we report a novel role for the actin cross-linking regulator filamin A (FLNa) in Vpu anti-tetherin activities. We demonstrate that FLNa associates with tetherin and that FLNa modulates tetherin turnover. FLNa deficiency was found to enhance cell surface and steady-state levels of tetherin expression. In contrast, we observed that overexpression of FLNa reduced tetherin expression levels both on the plasma membrane and in intracellular compartments. Although FLNb shows high amino acid sequence similarity with FLNa, we reveal that only FLNa, but not FLNb, plays an essential role in tetherin turnover. We further showed that FLNa deficiency inhibited Vpu-mediated enhancement of virus release through interfering with the activity of Vpu to down-regulate cellular tetherin. Taken together, our studies suggest that Vpu hijacks the FLNa function in the modulation of tetherin to neutralize the antiviral factor tetherin. These findings may provide novel strategies for the treatment of HIV-1 infection.

IFN-inducible bone marrow stromal antigen 2 (BST-2, also known as tetherin, CD317, and HM1.24) inhibits human immunodeficiency virus type 1 (HIV-1)[2] release and spreads by trapping newly formed virions on the surface of infected cells (1, 2). As an innate restriction factor, tetherin also exhibits antiviral activity against a wide range of enveloped viruses, such as filoviruses, arenaviruses, and herpesviruses (3–6). Tetherin is a 30- to 36-kDa glycosylated type II integral membrane protein (7). It has an unusual topology consisting of a short N-terminal cytoplasmic tail, a single transmembrane domain, an ectodomain with an extended coiled-coil structure stabilized by the formation of a homodimer through intermolecular disulfide bonds between any one of three conserved cysteine residues, and a C-terminal glycosylphosphatidylinositol anchor (8–11). Biochemical and microscopic studies support the hypothesis that two distinct membrane anchors and a coiled-coil conformation enable tetherin to restrict virus release through a direct tethering mechanism in which parallel tetherin dimers physically cross-link the virion and cell membranes (11–14).

Glycosylphosphatidylinositol-anchored tetherin associates with plasma membrane (PM) lipid rafts that serve as preferential sites of HIV-1 assembly and budding (8, 15). Also, tetherin has been found to be concentrated in internal compartments, including the trans-Golgi network, early endosomes, and recycling endosomes (8). Indeed, it has been documented that the membrane trafficking machinery is involved in tetherin transport and turnover. The clathrin-associated adaptor complex AP-2 mediates tetherin endocytosis via a direct interaction (16, 17). Internalized tetherin is then delivered to early endosomes and/or sorting endosomes from which tetherin is sorted for returning back to the PM via the recycling endosome pathway, is destined for degradation via endo-lysosomal pathways, or is targeted to trans-Golgi network compartments via a clathrin adaptor AP-1-mediated retrieval pathway (17–20).

In polarized epithelial cells, tetherin is mainly localized to the apical membrane through indirect interactions with the underlying actin cytoskeleton (21). Recent studies have also suggested that the linkage of tetherin with the cortical actin network plays a role in the organization of lipid rafts (22, 23). However, the mechanism of how the cortical actin network is involved in tetherin location and tetherin antiviral activity remains to be determined.

HIV-1 has evolved a strategy to overcome tetherin restriction by encoding the accessory viral protein U (Vpu). Vpu is a 16-kDa type I transmembrane protein composed of an N-terminal α-helical transmembrane domain and a C-terminal cytoplasmic domain that contains two α helices (H1 and H2) connected by an unstructured region harboring two evolutionary conserved serine residues. Vpu interaction with tetherin via their respective transmembrane domains is required for the Vpu activity to counteract tetherin restriction (24, 25). Multiple mechanisms of Vpu-mediated antagonism have been proposed. Vpu is capable of inhibiting the resupply of *de novo* synthesized tetherin and/or recycled tetherin to the PM

* This work was supported by National Institutes of Health Grants AI089330, MD007586, and MD007593 (to X. D.), AI080580 (to F. V.), and HL007737 and GM059994 (to D. D.). The authors declare that they have no conflicts of interest with the contents of this article. The content is solely the responsibility of the authors and does not necessarily represent the official views of the National Institutes of Health.

[1] To whom correspondence should be addressed: Dept. of Microbiology and Immunology and Center for AIDS Health Disparities Research, School of Medicine, Meharry Medical College, 1005 Dr. D. B. Todd Jr. Blvd., Nashville, TN 37208. Tel.: 615-327-6464; Fax: 615-327-6709; E-mail: xdong@mmc.edu.

[2] The abbreviations used are: HIV-1, human immunodeficiency virus, type 1; PM, plasma membrane; FLNa, filamin A; VLP, virus-like particle; ESCRT, endosomal sorting complex required for transport.

by sequestering it within the trans-Golgi network compartment (26, 27). Vpu can also induce tetherin degradation though the β-TrCP-dependent endo-lysosomal pathway (28). Recent studies support a mechanism by which Vpu can displace surface tetherin from virus budding sites (29, 30). Notably, these mechanisms are not mutually exclusive. It appears that Vpu is able to interfere with tetherin trafficking pathways to achieve its anti-tetherin activity. However, the exact mechanism of Vpu-mediated neutralization of tetherin is not well defined (31–33).

Here we report a novel role for the cytoskeletal protein filamin A (FLNa) in HIV-1 particle release through modulating tetherin expression. FLNa has an N-terminal conserved F-actin-binding domain followed by 24 immunoglobulin-like repeats with two calpain-sensitive unstructured hinge regions, 1 (separating repeats 15 and 16) and 2 (separating repeats 23 and 24). The extreme C-terminal repeat 24 of FLNa mediates dimerization via non-covalent interactions. FLNa links the cell membrane to the actin cytoskeleton and serves as a scaffold on which intracellular signaling and protein trafficking pathways are organized (34, 35). In this work, we show that FLNa involves tetherin turnover and trafficking pathways. Furthermore, we demonstrate that Vpu hijacks the FLNa function to antagonize tetherin restriction. Our findings provide novel insights into FLNa biology and Vpu-mediated evasion of host restriction.

Experimental Procedures

Cell Lines and Transfections—The human melanoma M2 and A7 cell lines, provided by Yasutaka Ohta and Thomas Stossel (Harvard Medical School, Boston, MA), were maintained in minimum essential medium supplemented with 8% newborn calf serum, 2% fetal calf serum, 100 units/ml penicillin, and 100 μg/ml streptomycin at 37 °C in 5% CO_2. A7 cells were cultured in the presence of 500 μg/ml G418. 293T and HeLa cells were obtained from the ATCC and maintained in Dulbecco's modified Eagle's medium supplemented with 10% fetal bovine serum, 100 units/ml penicillin, and 100 μg/ml streptomycin. M2, A7, and HeLa cells were transfected using Lipofectamine 2000 (Invitrogen). 293T cells were transfected using the polyethyleneimine method.

Plasmids—The FLNa-GFP expression plasmid pcDNA3-FLNa-GFP was provided by David Calderwood (Yale University, New Haven, CT) (36). The FLNb-GFP expression plasmid pCl-puro-FLNb-GFP was a gift from Arnoud Sonnenberg (The Netherlands Cancer Institute, Amsterdam, Netherlands) (37). An HA-tetherin expression plasmid was provided by Vincent Piguet (Cardiff University, Cardiff, UK) (38). The HIV-1 Gag-Pol expression plasmid pGPCINS was obtained from Xiao-Fang Yu (Johns Hopkins University, Baltimore, MD) (39). The full-length infectious HIV-1 molecular clone pNL4–3 and its Vpu-deficient variant pNL4–3/Udel have been described before (40, 41). A plasmid (pcDNA-Vphu) encoding the Vpu protein of HIV-1, NL4–3, was obtained through the National Institutes of Health AIDS Research and Reference Reagent Program (42). The plasmid (pcDNA3-myc-FLNa WT) encoding human FLNa fused with a myc tag was purchased from Addgene (Cambridge, MA) (43).

Primary Antibodies—Mouse anti-tetherin antibodies were provided by Chugai Pharmaceutical Co. (Kanagawa, Japan). Mouse anti-FLNa and anti-Myc antibodies were purchased from EMD Millipore (Billerica, MA). Mouse anti-HA antibodies were from Covance Co. (Princeton, NJ), mouse anti-GFP antibodies were from Invitrogen, and rabbit anti-FLNa antibodies were from Abcam. Rabbit anti-human tetherin antibodies, HIV-1 NL4–3 Vpu antiserum, HIV-Ig, and mouse anti-p24 antibodies (catalog no. 183-H12-5C) were obtained through the National Institutes of Health AIDS Research and Reference Reagent Program.

Co-immunoprecipitation—Co-immunoprecipitation assays were performed as described before (44). In brief, HeLa cells or 293T cells expressing FLNa-Myc and HA-tetherin were washed with phosphate-buffered saline and lysed with radioimmune precipitation buffer (150 mM NaCl, 1% Nonidet P-40, 1% sodium deoxycholate, 0.1% SDS, and 50 mM Tris-HCl (pH 7.6)). Cellular debris was removed from cell lysates by low-speed centrifugation, and the soluble cell lysate was then incubated overnight at 4 °C either with protein A/G-Sepharose beads (Thermo Fisher Scientific) alone or with the indicated antibodies and protein A/G-Sepharose beads. After washing with radioimmune precipitation assay buffer, immunoprecipitated proteins were subjected to SDS-polyacrylamide gel electrophoresis, followed by Western blotting with anti-Myc or anti-FLNa antibodies.

siRNA Knockdown—Three 21-nucleotide siRNA duplexes with symmetric 3′ UU overhangs were purchased from Thermo Fisher Scientific. Two FLNa-specific $siRNA_{FLNa\text{-}1}$ and $siRNA_{FLNa\text{-}2}$ sequences targeting the *FLNA* gene corresponded, respectively, to the coding regions 2555–2573 (CCAACAAGGTCAAAGTATA) and 2160–2178 (GCAGGAGGCTGGCGAGTAT) relative to the first nucleotide of the start codon. A control FLNa-nonspecific siRNA duplex ($siRNA_{control}$) was composed of a sense strand (5′-CUCUCGCCGUAAUAGCAGUUU-3′) and an antisense strand (5′-ACUGCUAUUACGGCGAGAGUU-3′). 100 nM siRNA duplexes were transfected into HeLa cells using Lipofectamine 2000.

Flow Cytometry—M2, A7, and transfected HeLa cells were stained with mouse anti-tetherin primary antibodies and goat anti-mouse IgG (H+L) APC-conjugated secondary antibodies. Cells were run on a BD Biosciences FACSCalibur flow cytometer, and the data were analyzed by FlowJo software.

Cycloheximide Treatment—M2 and A7 cells transfected with HA-tetherin or non-transfected M2 and A7 cells were preincubated for 2 h with 1.5 μg/ml cycloheximide (Sigma-Aldrich). Cells were then washed and incubated with 100 μg/ml cycloheximide for the indicated time, followed by immunoblot analysis with anti-HA, tetherin, and actin antibodies.

Immunofluorescence Microscopy—Immunofluorescence confocal microscopy was conducted as described previously (44). In single-staining experiments, endogenous tetherin or exogenously expressed HA-tetherin was detected by either mouse anti-tetherin or anti-HA antibodies and goat anti-mouse Alexa Fluor 546-conjugated antibodies (Life Technologies). In double-staining experiments, FLNa was stained with rabbit anti-FLNa antibodies and goat anti-rabbit Alexa Fluor 488-conjugated antibodies (Life Technologies). Tetherin

was revealed by mouse anti-tetherin antibodies and goat anti-mouse Alexa Fluor 546-conjugated antibodies. Images were acquired with either a Nikon TE2000U C1 confocal laser-scanning microscope or a Nikon AIR confocal microscope. Image analysis was performed using EZ-C1 and NIS-Elements AR software.

Purification of VLPs or Virions—In some experiments, A7 and M2 cells were cotransfected with HIV-1 Gag-Pol and tetherin expression plasmids at a ratio of 1:1. In some experiments, A7 and M2 cells were cotransfected with NL4–3/Udel proviral plasmids and HIV-1 Vpu expression plasmids. 48 h after transfection, supernatants were collected, filtered through a 0.45-μm filter, and purified through a 20% sucrose cushion by centrifugation at 28,000 $\times$ *g* for 2 h at 4 °C.

Results

FLNa Down-regulates Tetherin Expression—Our previous studies have demonstrated that FLNa binds HIV-1 Gag and promotes the transport of the latter protein to the PM (44). To further define the role of FLNa in HIV-1 particle release, we performed transmission electron microscopy to observe virus budding events in an FLNa-depleted human melanoma cell line (M2) and its derivative rescued subline (A7) stably expressing FLNa at approximately wild-type levels (45). In A7 cells, cell-free virions surrounding the PM were detected easily. Although fewer virions were found at the cell surface of M2 cells, we observed some virions tethered to each other and to the cell surface (data not shown). A retention phenotype occurred in M2 cells but not in A7 cells, suggesting that FLNa depletion may result in the accumulation of tetherin on the cell surface. To test this possibility, we performed flow cytometry in non-permeabilized A7 and M2 cells to quantify tetherin expression on the cell surface. As expected, cell surface tetherin levels in M2 cells increased 2-fold compared with A7 cells (Fig. 1*A*). To determine whether a reduction in surface tetherin expression in A7 cells resulted from lower levels of total cellular tetherin, we conducted a Western blotting analysis of extracts from these two cell lines. Tetherin is a 30- to 36-kDa type II transmembrane glycoprotein (7, 8). Indeed, A7 cells exhibited a lower level of endogenously expressed tetherin compared with M2 cells (Fig. 1*B*). Similarly, in cells transfected with HA-tetherin expression plasmids, M2 but not A7 cells showed a higher level of exogenously expressed HA-tetherin (Fig. 1*C*). All of these results indicate that FLNa promotes tetherin down-regulation. To confirm these findings, we performed rescue experiments in M2 cells. M2 cells were transfected with either control plasmids or full-length FLNa expression plasmids. The transient expression of FLNa in M2 cells not only reduced total cellular tetherin expression (Fig. 1*D*) but also decreased the level of cell surface tetherin (data not shown). To exclude the possibility that the observed difference in endogenous and/or exogenous tetherin expression levels is the consequence of clonal selection during the generation of M2 and A7 cell lines, we performed an siRNA approach in HeLa cells. Expression of FLNa-specific siRNA in HeLa cells, either $siRNA_{FLNa\text{-}1}$ or $siRNA_{FLNa\text{-}2}$, efficiently decreased total cellular levels of endogenous FLNa by more than 80% compared with expression of control siRNA (Fig. 1*E*). siRNA-mediated knockdown of FLNa enhanced the levels of cellular tetherin (Fig. 1*E*) and surface tetherin (Fig. 1*F*). To further evaluate the relationship between FLNa and tetherin, we compared FLNa and tetherin levels in Jurkat and THP-1 cells. Jurkat cells with higher levels of FLNa exhibited lower expression of tetherin compared with THP-1 cells (data not shown). Taken together, these data suggest that FLNa normally acts to promote tetherin down-modulation.

FLNa Depletion Reduces Tetherin Turnover—To investigate a potential role for FLNa in promoting tetherin deregulation, we tested whether FLNa deficiency decreases tetherin turnover. To that end, HA-tetherin-expressing M2 and A7 cells were incubated in growth medium supplemented with cycloheximide at different time intervals, followed by immunoblot analysis for HA-tetherin expression. In our experiments, HA-tetherin in A7 and M2 cells appeared as a smear of 28–45 kDa. Our results showed that FLNa depletion in M2 cells extended the half-life of HA-tetherin, thereby stabilizing HA-tetherin expression (Fig. 2*A*). To quantify the half-life of endogenous tetherin, we performed cycloheximide chase experiments in non-transfected M2 and A7 cells. In A7 cells, more than 50% of tetherin was degraded 3 h after cycloheximide treatment (Fig. 2*B*, *left panel*). By contrast, only 20% of tetherin in M2 cells was degraded at this time point (Fig. 2*B*, *right panel*). Quantification of a tetherin band at about 30–36 kDa using densitometry showed that FLNa deficiency in M2 cells extended the half-life of endogenous tetherin as compared with A7 cells (Fig. 2*C*). These results indicate that FLNa promotes tetherin turnover.

FLNb Is Not Required for Tetherin Turnover—Given that FLNa depletion increased tetherin expression, we reasoned that enhanced FLNa may reduce tetherin levels. To test this possibility, HeLa cells were transfected with either control pcDNA3.1 empty plasmids or FLNa-GFP expression plasmids. Indeed, expression of FLNa-GFP reduced total cellular tetherin levels 2-fold (Fig. 3*A*). To determine the effect of FLNa-GFP expression on cell surface tetherin, we performed similar experiments in HeLa cells, and surface tetherin levels on either FLNa-GFP-positive cells or FLNa-GFP-negative cells were then quantified by flow cytometry. As shown in Fig. 3*B*, a 2-fold reduction in surface tetherin levels was detected in FLNa-GFP-expressing cells. Considering that FLNb and FLNa are the most ubiquitously expressed filamin isoforms and that FLNb shares ~70% amino acid sequence homology with FLNa, we examined whether FLNb also participates in the modulation of tetherin (46–48). In that regard, HeLa cells were transfected with either empty pcDNA3.1 vectors or FLNb-GFP expression plasmids. In contrast to FLNa-GFP-induced down-regulation of tetherin, FLNb-GFP expression did not alter total cellular total levels of tetherin (Fig. 3*C*). Furthermore, flow cytometric analysis of FLNb-GFP-expressing HeLa cells showed that the cell surface tetherin levels were comparable with those in FLNb-GFP-negative cells (Fig. 3*D*). Collectively, these results indicate that the isoform-specific regulation of tetherin modulation is mediated by FLNa but not FLNb.

FLNa Associates with Tetherin in Mammalian Cells—To understand the molecular mechanism of FLNa-mediated modulation of tetherin, we first performed co-immunoprecipitation assays in mammalian cells. Vpu-permissive 293T cells, which

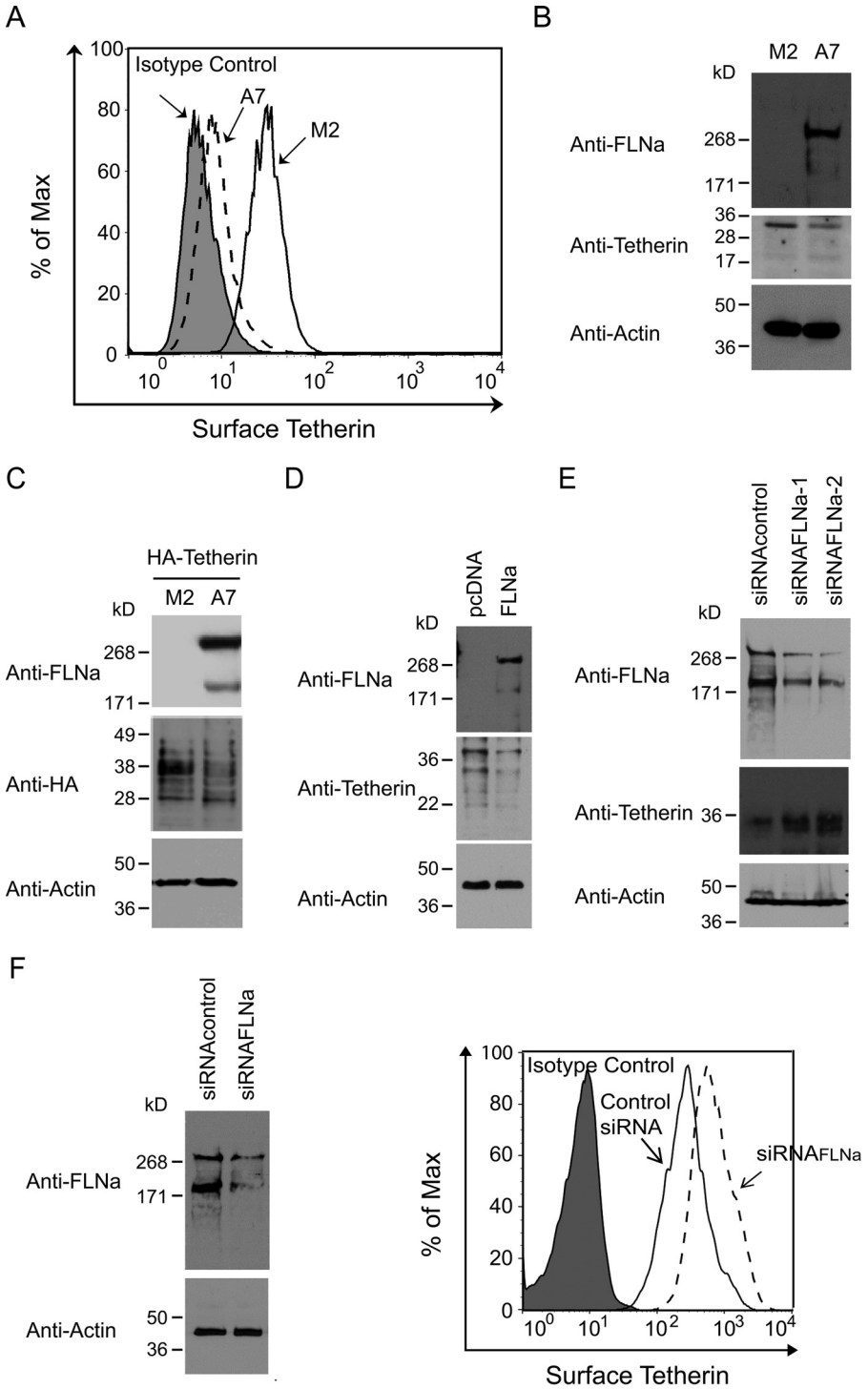

FIGURE 1. **FLNa closely correlates with tetherin expression levels.** *A*, flow cytometric analysis of surface tetherin levels on M2 and A7 cells. The *filled plot* represents the isotype control, the *dashed plot* represents A7 cells, and the *empty plot* represents M2 cells. *B*, Western blotting analysis of M2 and A7 cell lysates using anti-FLNa, anti-tetherin, and anti-tubulin antibodies. *C*, immunoblot analysis of HA-tetherin-expressing M2 and A7 cells with anti-FLNa, anti-HA, and anti-actin antibodies. *D*, M2 cells were transfected with empty pcDNA vectors or full-length FLNa expression plasmids, followed by Western blotting analysis with anti-FLNa, anti-tetherin, and anti-actin antibodies. *E*, HeLa cells were transfected with $siRNA_{control}$, $siRNA_{FLNa-1}$, or $siRNA_{FLNa-2}$. 48 h after transfection, cells were lysed and subjected to immunoblot analysis using anti-FLNa, anti-tetherin, and anti-actin antibodies. *F*, HeLa cells were transfected with $siRNA_{control}$ or $siRNA_{FLNa}$. 40 h after transfection, cells were lysed, followed by immunoblot analysis using anti-FLNa and anti-actin antibodies, or cells were subjected to flow cytometric analysis of surface tetherin. The *filled plot* represents the isotype control, the *empty plot* represents cells receiving control siRNA, and the *dashed plot* represents cells receiving $siRNA_{FLNa}$.

do not express tetherin, were co-transfected with an expression plasmid encoding FLNa with a C-terminal Myc tag and an expression plasmid encoding HA-tagged tetherin at a ratio of 1:1. HA-tetherin, precipitated by anti-HA antibodies and protein G-coupled Sepharose beads, interacted with FLNa-Myc (Fig. 4*A*). Similarly, co-immunoprecipitation of HA-tetherin

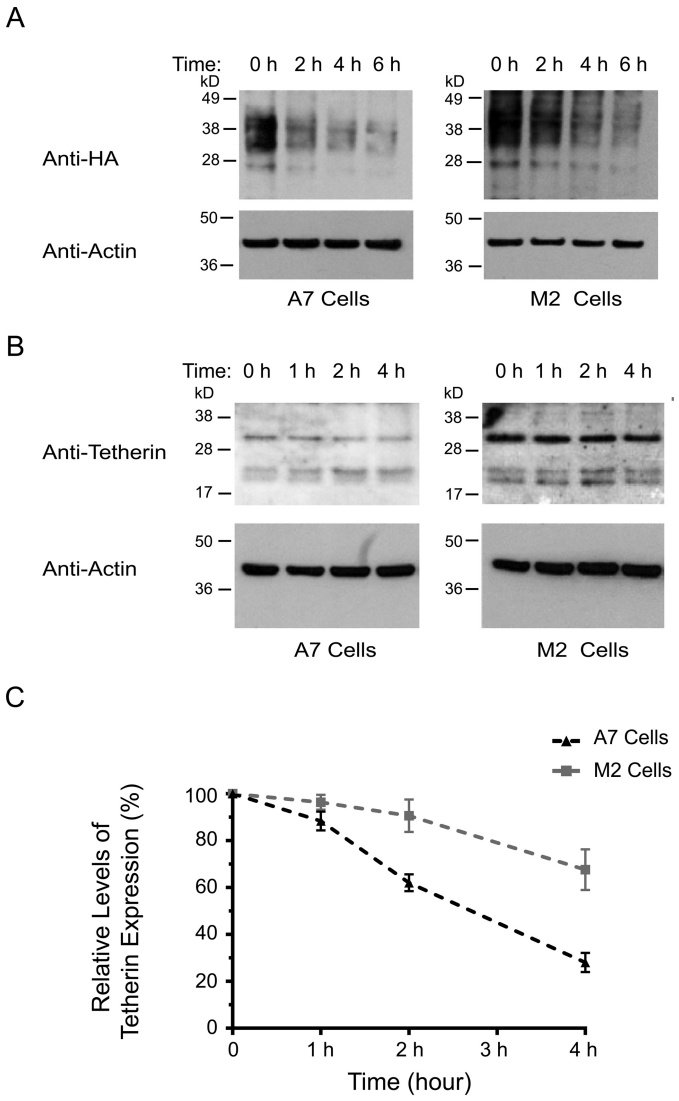

FIGURE 2. **FLNa depletion stabilizes tetherin expression.** *A*, HA-tetherin-expressing A7 (*left panel*) and M2 (*right panel*) cells were treated with cycloheximide for the indicated times (0, 2, 4, and 6 h), followed by Western blotting analysis with antibodies against HA and actin. *B*, A7 (*left panel*) and M2 (*right panel*) cells were treated with cycloheximide for the indicated times (0, 1, 2, and 4 h), followed by immunoblot analysis using anti-tetherin and anti-actin antibodies. *C*, densitometry values of tetherin (about 30–36 kDa) signal intensities at each time point normalized to the densitometry value at the first time point, which was set to 100%. The results shown represent the mean ± S.D. ($n = 3$).

with endogenous FLNa was also detected in 293T cells expressing HA-tagged tetherin.[3] To confirm these results, we conducted co-immunoprecipitation experiments in Vpu-restrictive HeLa cells, which express tetherin constitutively. As shown in Fig. 4*B*, cellular tetherin co-immunoprecipitated with endogenous FLNa. We next performed immunofluorescence confocal microscopy to examine whether tetherin co-localized with FLNa. In HeLa cells, endogenous FLNa and native tetherin were found to primarily locate at the PM (Fig. 4*C*). Moreover, a high level of FLNa-tetherin colocalization was detected at distinct regions of the PM (Fig. 4*C*). Taken together, these results suggest that FLNa associates with tetherin in mammalian cells.

[3] D. Dotson, E. A. Woodruff, F. Villalta, and X. Dong, unpublished data.

FLNa Is Involved in the Tetherin Trafficking Pathway—FLNa, as an actin-cross-linking protein, is implicated in the intracellular trafficking pathways of some membrane proteins (44, 49–52). However, whether FLNa regulates tetherin subcellular trafficking is unknown. To explore this possibility, we examined the role of FLNa in tetherin subcellular localization by performing immunofluorescence confocal microscopy. We first observed the distribution pattern of endogenous tetherin in A7 and M2 cells (Fig. 5*A*). In A7 cells, endogenous tetherin was concentrated in the perinuclear region (Fig. 5*A*, *left panels*). By contrast, endogenous tetherin in M2 cells was localized both on the PM and in intracellular compartments (Fig. 5*A*, *right panels*). We also examined the subcellular localization of exogenously expressed HA-tetherin in these two cell lines. Similar to endogenous tetherin, HA-tetherin in A7 cells was primarily localized in the perinuclear compartment, whereas, in M2 cells, HA-tetherin showed an intracellular punctate and PM pattern (Fig. 5*B*). The distinct distribution patterns of tetherin in cells in the presence or absence of FLNa suggest that FLNa participates in the tetherin trafficking pathway. In these experiments, we failed to observe PM localization of either endogenous tetherin or exogenously expressed HA-tetherin in A7 cells. However, the flow cytometric analysis of non-permeabilized A7 cells showed the presence of cell surface tetherin (Fig. 1*A*). These inconsistent results in cell surface tetherin expression may be partially caused by the anti-tetherin antibodies we used that might exhibit a reduced binding efficiency to cell surface tetherin on fixed and permeabilized A7 cells. Next we investigated the effect of FLNa overexpression on the localization of endogenous tetherin. To that end, HeLa cells were transfected with FLNa-GFP expression plasmids, followed by immunofluorescence confocal microscopy. In cells devoid of FLNa-GFP expression, tetherin was localized both on the PM and in perinuclear regions. In cells expressing FLNa-GFP, however, the fluorescence intensity of tetherin staining on the PM and perinuclear region was reduced significantly (Fig. 5*C*). As controls, we also examined HeLa cells in the presence of FLNb-GFP. FLNb-GFP was detected predominantly on the PM and exhibited high levels of co-localization with tetherin. In contrast to FLNa-GFP, the presence of FLNb-GFP did not induce a reduction in tetherin fluorescence on the PM and in the perinuclear region (Fig. 5*D*). Taken together, these results reveal that FLNa plays a role in tetherin intracellular trafficking.

FLNa Is Required for HIV-1 Vpu-mediated Enhancement of Virus Release—It is well known that PM-localized tetherin restricts the release of HIV-1 particles by cross-linking nascent viral and cellular membranes (11, 53). To determine the role of FLNa in tetherin antiviral activity, either A7 cells or M2 cells were co-transfected with HIV-1 Gag-Pol and tetherin expression plasmids. Considering cell line-dependent differences in transfection efficiency because of cell surface morphology, we compared Gag-Pol virus-like particle (VLP) release from A7 cells with *versus* without exogenously expressed tetherin, or from M2 cells with *versus* without exogenously expressed tetherin. In FLNa-repleted A7 cells, exogenous expression of tetherin efficiently inhibited the release of Gag-Pol VLPs (Fig. 6*A*). Similarly, forced expression of tetherin in FLNa-deficient M2 cells also restricted HIV-1 Gag-Pol VLP release (Fig. 6*B*). These

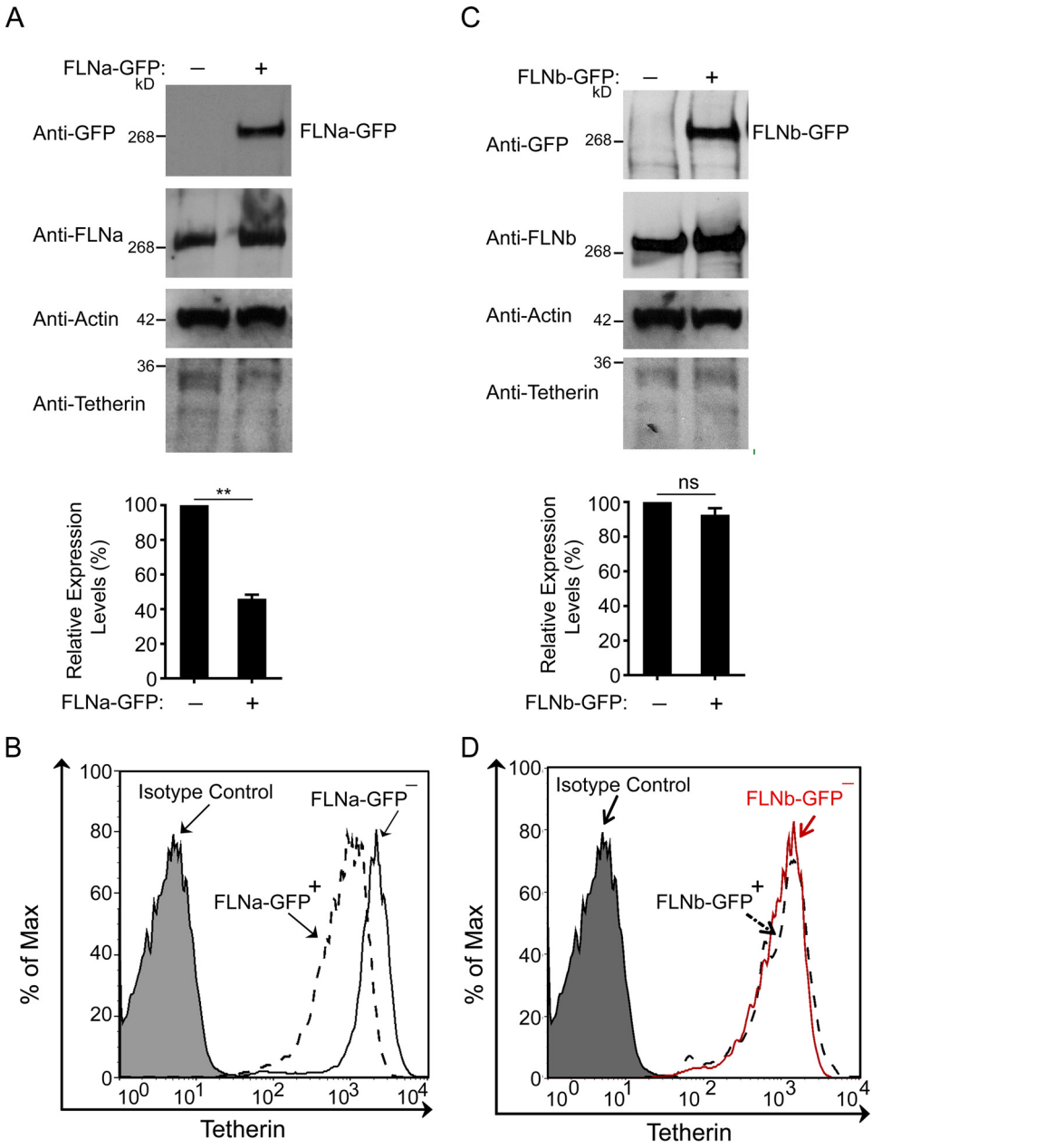

FIGURE 3. **FLNb overexpression does not affect tetherin expression.** *A*, HeLa cells were transfected with either empty pcDNA3.1 vectors or FLNa-GFP expression plasmids, followed by Western blotting with the indicated antibodies. The graph below the blots represent the densitometric value of tetherin signal intensities normalized to the densitometric value of the *left lane* set to 100 (**, $p < 0.01$). The results shown represent the mean ± S.D. ($n = 4$). *B*, HeLa cells were transfected with FLNa-GFP expression plasmids. 48 h after transfection, non-permeabilized cells were immunostained for cell surface tetherin. Gating was performed on FLNa-GFP-positive and FLNa-GFP-negative cells. The *filled plot* represents the isotype control, the *dashed plot* represents FLNa-GFP-expressing cells, and the *empty plot* represents cells in the absence of FLNa-GFP. *C*, HeLa cells were cotransfected with empty pcDNA3.1 vectors and FLNb-GFP expression plasmids. Transfected cells were then subjected to immunoblot analysis with the indicated antibodies. The graph below represents densitometric values of blots showing tetherin signal intensities normalized to densitometric values of the *left lane* set to 100 (*ns*, no significance). The results shown represent the mean ± S.D. ($n = 4$). *D*, HeLa cells were transfected with FLNb-GFP expression plasmids, followed by flow cytometric analysis of surface tetherin on cells either expressing FLNb-GFP (*dashed plot*) or non-expressing FLNb-GFP (*red plot*). The *filled plot* represents the isotype control.

results suggest that FLNa depletion does not impair trafficking of *de novo* synthesized tetherin to the PM. Next we examined the effect of FLNa on Vpu-mediated enhancement of HIV-1 release. To that end, Vpu-defective NL4–3 (NL4–3/Udel) and HIV-1 Vpu were co-expressed in A7 or M2 cells. As a control, the presence of Vpu in A7 cells effectively increased the release of NL4–3/Udel viruses (Fig. 6*C*). By contrast, expression of Vpu in *trans* in M2 cells, even at higher levels, did not induce an increase in NL4–3/Udel yield (Fig. 6*D*). These data indicate that FLNa depletion inhibits the activity of Vpu to enhance HIV-1 particle release. Indeed, the presence of Vpu in A7 cells significantly reduced tetherin expression levels, whereas Vpu expression in M2 cells did not induce a reduction in total cellular tetherin expression (data not shown). It suggests that FLNa deficiency impairs the activity of Vpu to down-regulate tetherin, thereby inhibiting the

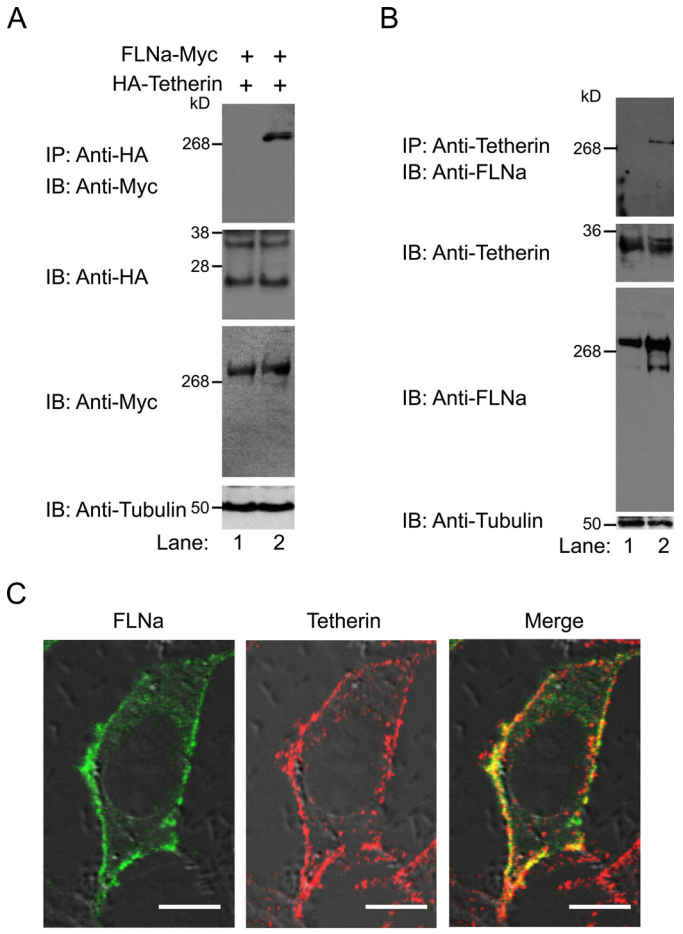

FIGURE 4. **FLNa associates with tetherin in mammalian cells.** *A*, FLNa-Myc and HA-tetherin co-expressing 293T cells were incubated with either protein G-agarose alone (*lane 1*) or protein G-agarose and anti-HA antibodies (*lane 2*), followed by immunoblot (*IB*) analysis with anti-Myc antibodies. Cell lysates before immunoprecipitation (*IP*) were probed with anti-HA, anti-Myc, and anti-tubulin antibodies. *B*, HeLa cell lysates were incubated with either protein G-agarose alone (*lane 1*) or protein G-agarose and anti-tetherin antibodies (*lane 2*), followed by Western blotting analysis using anti-FLNa antibodies. Cell lysates before immunoprecipitation were subjected to immunoblot analysis with anti-tetherin, anti-FLNa, and anti-tubulin antibodies. *C*, confocal immunofluorescence microscopy examination of FLNa colocalization with tetherin. HeLa cells grown overnight were fixed, permeabilized, and immunostained for FLNa and tetherin. FLNa is shown in *green* (*left panel*), tetherin in *red* (*center panel*), and co-localized pixels in *yellow* (*right panel*). *Scale bars* = 10 μm.

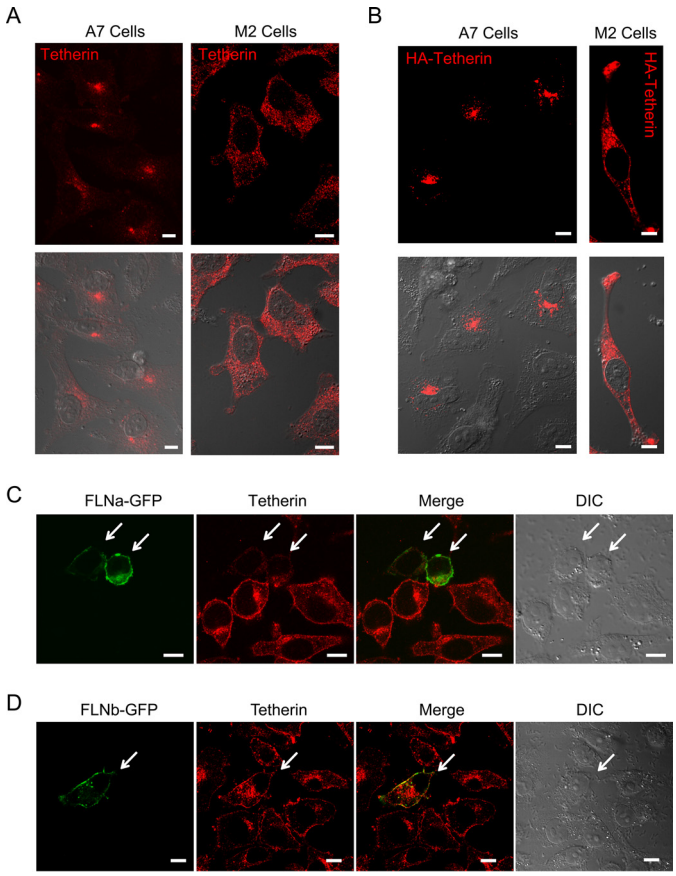

FIGURE 5. **FLNa is involved in tetherin trafficking pathways.** *A*, distribution pattern of endogenous tetherin in A7 (*left panels*) and M2 (*right panels*) cells. Tetherin is shown in *red*. Differential interference contrast images merged with confocal images of tetherin are shown in the *bottom panels*. *Scale bars* = 10 μm. *B*, distribution pattern of exogenously expressed HA-tetherin in A7 (*left panels*) and M2 (*right panels*) cells. HA-tetherin was detected by anti-HA antibodies and fluorescent secondary antibodies. HA-tetherin is shown in *red*. Differential interference contrast images merged with confocal images of HA-tetherin are shown in the *bottom panels*. *Scale bars* = 10 μm. *C* and *D*, HeLa cells were transfected with FLNa-GFP (*C*) or FLNb-GFP (*D*) expression plasmids. Transfected cells were then immunostained for endogenous tetherin. FLNa-GFP or FLNb-GFP is shown in *green* (*first panel*), tetherin in *red* (*second panel*), and the co-localized pixels in *yellow* (*third panel*). A differential interference contrast image is shown in the *fourth panel*. Cells expressing either FLNa-GFP (*C*) or FLNb-GFP (*D*) are indicated by *arrows*. *Scale bars* = 10 μm.

virus release activities of Vpu. Taken together, these results demonstrate that FLNa is involved in Vpu antagonism of tetherin restriction.

Discussion

In this study, we demonstrate that the actin-binding protein FLNa plays an important role in modulating tetherin expression at a posttranslational level. Employing an FLNa-depleted human melanoma cell line and its subline with stable expression of recombinant FLNa, we found that FLNa deficiency increased surface and total cellular tetherin levels, whereas FLNa repletion reduced surface and cellular tetherin expression. FLNa-induced down-regulation of surface and cellular tetherin was confirmed further in HeLa cells with either FLNa knockdown or FLNa overexpression. Coupled with evidence showing that the presence of FLNa is required for the activity of HIV-1 Vpu to enhance virus release, it suggests that HIV-1 Vpu hijacks the FLNa function of regulating tetherin expression levels to enhance HIV-1 particle release.

The presence and absence of FLNa in melanoma cells led to the distinct distribution patterns of endogenous and exogenously expressed tetherin, highlighting the importance of FLNa in tetherin trafficking and location. Indeed, increasing evidence indicates that FLNa regulates the transport of ion channels and transmembrane receptors into or out of the PM via the endocytic pathway and/or secretory pathway (51, 54–56). Our microscopy studies showing that enhanced FLNa expression reduced tetherin localization on the PM, together with two lines of evidence of FLNa co-immunoprecipitation with tetherin and FLNa colocalization with tetherin on the PM, suggest that FLNa may promote tetherin internalization. In support of this, exogenously expressed tetherin in M2 cells still exhibited anti-viral activities, implying that FLNa depletion does not

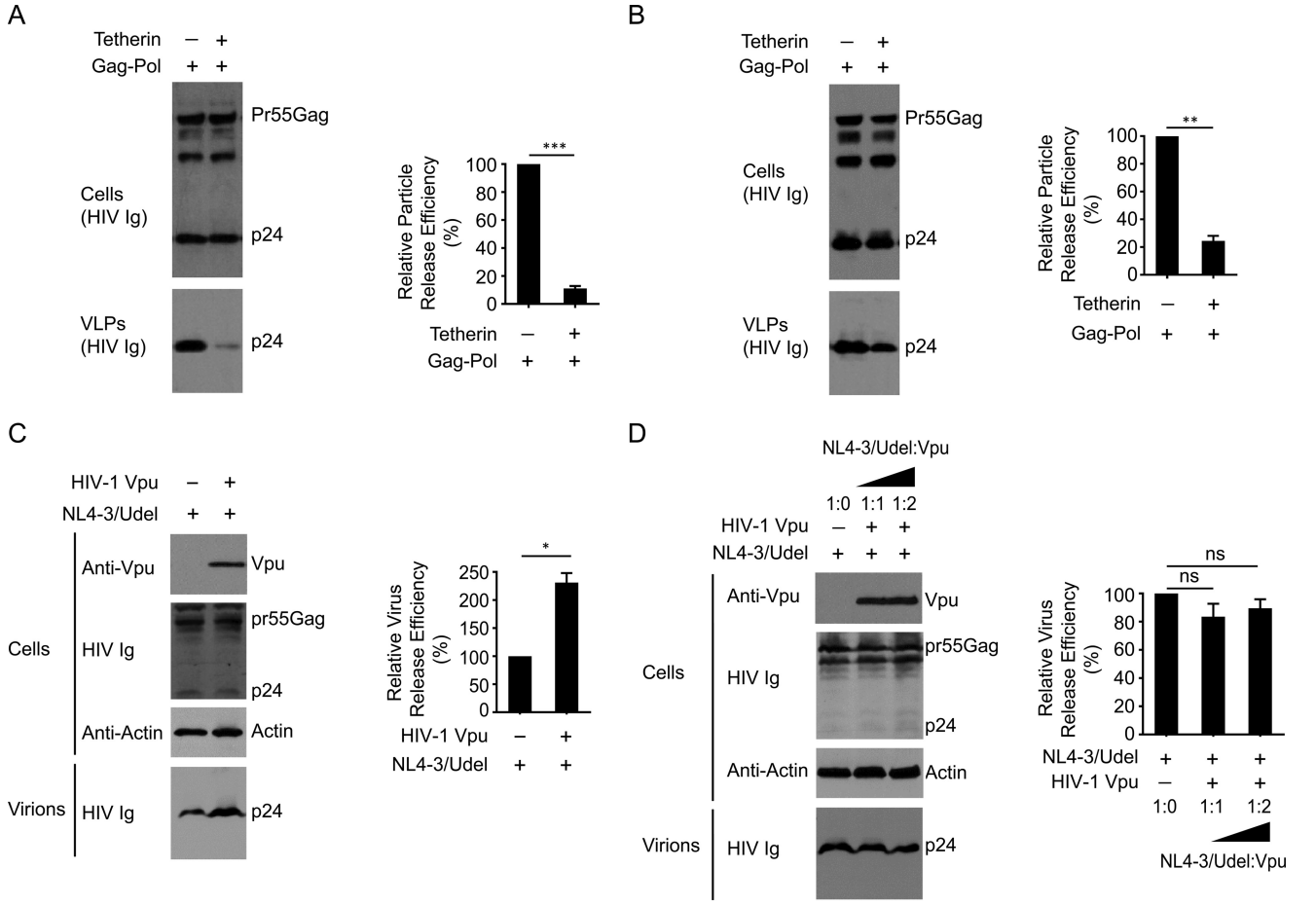

FIGURE 6. **FLNa depletion inhibits the activity of HIV-1 Vpu to enhance virus release.** *A* and *B*, A7 cells (*A*) or M2 cells (*B*) were cotransfected with HIV-1 Gag-Pol and tetherin expression plasmids at a ratio of 1:1, followed by Western blotting analysis of cell lysates and pelleted VLP lysates using HIV Ig. The *right panels* represent relative particle release efficiency (**, $p < 0.01$; ***, $p < 0.001$). Relative particle release efficiency was determined as p24 levels in the supernatant as a fraction of total p24 levels (supernatant plus cell lysates) and normalized to the particle release efficiency in A7 (*A*) or M2 (*B*) cells expressing HIV-1 Gag-Pol alone. The results shown represent the mean ± S.D. ($n = 3$). *C*, A7 cells were cotransfected with Vpu-defective NL4–3 proviral plasmids (NL4–3/Udel) and either empty pcDNA3.1 vectors or HIV-1 Vpu expression plasmids, followed by immunoblot analysis of cell lysates (anti-Vpu antibodies, HIV Ig, and anti-actin antibodies) and virion lysates (HIV Ig). The *right panel* represents relative particle release efficiency (*, $p < 0.1$). Relative virus release efficiency was determined as p24 levels in the supernatant as a fraction of total p24 levels (supernatant plus cell lysates) and normalized to the virus release efficiency in A7 cells only expressing NL4–3/Udel. The results shown represent the mean ± S.D. ($n = 3$). *D*, M2 cells were cotransfected with NL4–3/Udel and HIV-1 Vpu expression plasmids at different ratios (from 1:0 to 1:2), followed by Western blotting analysis of cell lysates (anti-Vpu antibodies, HIV Ig, and anti-actin antibodies) and virion lysates (HIV Ig). The *right panel* represents relative particle release efficiency (*ns*, no significance). Relative virus release efficiency was determined as p24 levels in the supernatant as a fraction of total p24 levels (supernatant plus cell lysates) and normalized to virus release efficiency in M2 cells only expressing NL4–3/Udel. The results shown represent the mean ± S.D. ($n = 3$).

interfere with the transport of *de novo* synthesized tetherin to assembly sites of HIV-1. It is well known that FLNa binds diverse ion channels and transmembrane receptors via repeats 16–23 (57). In agreement with this view, our early studies have demonstrated that FLNa repeats 16–23 are required for binding to HIV-1 Gag (44). Whether FLNa repeats 16–23 are involved in tetherin binding remains to be determined.

PM-localized tetherin is concentrated within the lipid rafts because of the C-terminal glycosylphosphatidylinositol modification (8, 17). The adaptor complex AP-2 recognizes a non-canonical dual tyrosine motif in the tetherin cytosolic tail and mediates tetherin endocytosis through a clathrin-dependent mechanism (16, 17). Interestingly, the Rho GTPase-activating protein RICH2 has been reported recently to interact with this tyrosine-based motif and link tetherin to the actin cytoskeleton via the proteins EBP50 and erzin (21). Such a linkage is implicated both in the organization of PM lipid raft microdomains by limiting the free diffusion of membrane lipids and proteins and in the remodeling of actin dynamics by regulating the small GTPases Rho and/or Rac (21–23). Notably, it has been reported that RICH2 binding prevented tetherin from interacting with AP-2 and, therefore, inhibited clathrin-dependent endocytosis of tetherin (21). Further investigations are needed to determine the mechanisms of how these two mutually competitive interactions are orchestrated under physiological conditions.

Our early studies in M2 cells using a transferrin uptake assay indicate that FLNa deficiency does not perturb clathrin-mediated constitutive endocytosis of transferrin, suggesting that FLNa may contribute to a clathrin-independent pathway required for tetherin internalization (44). Indeed, FLNa is implicated in promoting the internalization of the caveola-associated protein caveolin 1 (Cav-1) through a direct interaction with Cav-1 (51, 58, 59). The structural properties of FLNa, featured with two actin binding domains (in the N terminus and in

linear repeats 1–15) and one C-terminal self-association domain, enables it to cross-link the actin cytoskeleton into orthogonal branches (35). FLNa-dependent connections of Cav-1 to the actin cytoskeleton have been reported to be required both for the proper organization of Cav-1-associated membrane domains and for the regulation of caveola dynamics (59). Similar to tetherin, Cav-1 exhibited the distinct distribution patterns in M2 *versus* A7 cells (51). Coupled with early evidence of partial colocalization of tetherin with Cav-1 on the PM (8), this suggests that FLNa-dependent connections of tetherin to the actin cytoskeleton may facilitate tetherin clustering into Cav-1-enriched membrane domains and, therefore, promote its endocytosis through a caveolin-dependent pathway. It is noted that this model does not negate the role of the clathrin-dependent pathway in the constitutive endocytosis of tetherin. Indeed, FLNa-depleted M2 cells still exhibited tetherin localization in internal compartments, indicating that FLNa deficiency does not completely block tetherin endocytosis through the AP-2-mediated pathway. In the tetherin cytoplasmic tail, non-canonical dual tyrosine residues (Y^6XY^8) have been reported to be essential for the binding of the AP-2 complex that directs tetherin endocytosis (16, 17). This motif is also implicated in the binding of the AP-1 complex that regulates tetherin retrieval transport (21). The role of this motif in tetherin association with FLNa remains unknown. However, there exists a possibility that FLNa-bound tetherin may induce the exposure of the Y^6XY^8 motif, which can be efficiently recognized by AP-2 and AP-1 complexes. Further studies are warranted to define the relative importance of the AP-2-mediated constitutive pathway *versus* the FLNa-dependent regulated pathway on tetherin endocytosis.

Membrane pathways have been implicated in tetherin trafficking (16, 17). When endocytosed, tetherin can be recycled back to the PM via early endosomes/sorting endosomes, recycling endosomes, or the trans-Golgi network compartment or can be targeted for degradation via lysosomes or proteasomes (60, 61). Several lines of evidence indicate that the endo-lysosomal pathway is required for tetherin turnover through an ubiquitin-dependent manner (62, 63). Indeed, the ESCRT-0 subunit hepatocyte growth factor-regulated tyrosine kinase substrate is implicated both in recognizing ubiquitinated tetherin and in targeting tetherin for lysosomal degradation via an ESCRT-dependent mechanism (19). An ESCRT-I subunit, ubiquitin associated protein 1 (UBAP1), has been reported to be responsible for tetherin degradation in the multivesicular body pathway (64, 65). Furthermore, perturbation of Rab7A function in the late endocytic pathway prevents tetherin from degradation, supporting that lysosomal targeting of tetherin contributes to, at least in part, its constitutive turnover (20). Considering the results showing that either FLNa deficiency or FLNa overexpression induced an alteration in tetherin expression levels, we propose that FLNa targets endocytosed tetherin to the endo-lysosomal pathway for degradation. This hypothesis is supported by recent studies indicating that a portion of internalized Cav-1 is ubiquitinated and targeted to the degradation pathway through an ESCRT-dependent mechanism (66).

HIV-1 Vpu interaction with tetherin via their respective transmembrane domains is believed to be essential for Vpu to counteract tetherin antiviral activity (29, 67–69). It is clear that Vpu removes tetherin from sites of virus budding. However, the exact mechanism of Vpu-mediated antagonism is still under debate (70–72). It has been shown that casein kinase II-mediated phosphorylation facilitates Vpu interaction with β-TrCP and, therefore, recruitment of the Skp1·Cul1·F-box E3 ubiquitin ligase complex, which induces tetherin ubiquitination and degradation via an endo-lysosomal pathway (28, 73, 74). In some cell types, however, it has been suggested that Vpu can hijack AP-1 function in the retrograde transport of tetherin and, therefore, sequester tetherin in the perinuclear compartment (26, 27, 75, 76). In addition, recent studies support a third mechanism by which membrane anchoring of Vpu via its N-terminal tryptophan residue can displace tetherin from sites of virus assembly (29, 30). It is noted that these mutually non-exclusive mechanisms may be involved in the neutralization of tetherin either in a parallel manner or in a cell type-dependent manner. Our virological studies in A7 cells with FLNa expression support the view that virus release activity of Vpu in melanoma cells is achieved by down-regulating tetherin. However, FLNa deficiency in this cell type disables the activities of Vpu to down-modulate tetherin and to enhance virus release, implicating the involvement of FLNa in the Vpu antagonism of tetherin restriction. Taken together, these results suggest that Vpu-mediated evasion of tetherin restriction is required for FLNa function in tetherin internalization and down-regulation, although the underlying mechanism remains to be determined. Of note, two possibilities should be considered. The first one is that FLNa association with tetherin may induce a conformational change in tetherin that can be targeted efficiently by Vpu. The second mechanism is that FLNa-dependent trafficking pathways of tetherin are impaired by Vpu. Therefore, FLNa deficiency may sequester tetherin from Vpu, inhibiting Vpu anti-tetherin activities.

In summary, we showed that FLNa is involved in tetherin down-regulation and degradation and in the Vpu-mediated enhancement of virus release. Our results link the actin cytoskeleton to FLNa subcellular trafficking. These studies provide new insights into the Vpu-mediated neutralization of tetherin.

Author Contributions—D. D. performed the research and analyzed the data. E. A. W. provided technical support for the transmission electron microscopy experiments. F. V. contributed new reagents. X. D. designed the research, analyzed the data, and wrote the paper with input from F. V. and D. D.

Acknowledgments—We thank David Calderwood, Fumihiko Nakamura, Yasutaka Ohta, Vincent Piguet, Arnoud Sonnenberg, Thomas Stossel, and Xiao-Fang Yu for reagents. The following reagents were obtained through the National Institutes of Health AIDS Research and Reference Reagent Program: pNL4–3 from Malcolm Martin, pcDNA-Vphu from Stephan Bour and Klaus Strebel, anti-human BST-2 from Klaus Strebel and Amy Andrew, HIV-IG from Luiz Barbosa, and HIV-1 p24 monoclonal antibody from Bruce Chesebro and Kathy Wehrly. We thank the Meharry Morphology Core and FACS Core for assistance with confocal microscopy and flow cytometry.

References

1. Neil, S. J., Zang, T., and Bieniasz, P. D. (2008) Tetherin inhibits retrovirus release and is antagonized by HIV-1 Vpu. *Nature* **451,** 425–430
2. Van Damme, N., Goff, D., Katsura, C., Jorgenson, R. L., Mitchell, R., Johnson, M. C., Stephens, E. B., and Guatelli, J. (2008) The interferon-induced protein BST-2 restricts HIV-1 release and is downregulated from the cell surface by the viral Vpu protein. *Cell Host Microbe* **3,** 245–252
3. Jouvenet, N., Neil, S. J., Zhadina, M., Zang, T., Kratovac, Z., Lee, Y., McNatt, M., Hatziioannou, T., and Bieniasz, P. D. (2009) Broad-spectrum inhibition of retroviral and filoviral particle release by tetherin. *J. Virol.* **83,** 1837–1844
4. Sakuma, T., Noda, T., Urata, S., Kawaoka, Y., and Yasuda, J. (2009) Inhibition of Lassa and Marburg virus production by tetherin. *J. Virol.* **83,** 2382–2385
5. Kaletsky, R. L., Francica, J. R., Agrawal-Gamse, C., and Bates, P. (2009) Tetherin-mediated restriction of filovirus budding is antagonized by the Ebola glycoprotein. *Proc. Natl. Acad. Sci. U.S.A.* **106,** 2886–2891
6. Mansouri, M., Viswanathan, K., Douglas, J. L., Hines, J., Gustin, J., Moses, A. V., and Früh, K. (2009) Molecular mechanism of BST2/tetherin downregulation by K5/MIR2 of Kaposi's sarcoma-associated herpesvirus. *J. Virol.* **83,** 9672–9681
7. Ishikawa, J., Kaisho, T., Tomizawa, H., Lee, B. O., Kobune, Y., Inazawa, J., Oritani, K., Itoh, M., Ochi, T., and Ishihara, K. (1995) Molecular cloning and chromosomal mapping of a bone marrow stromal cell surface gene, BST2, that may be involved in pre-B-cell growth. *Genomics* **26,** 527–534
8. Kupzig, S., Korolchuk, V., Rollason, R., Sugden, A., Wilde, A., and Banting, G. (2003) Bst-2/HM1.24 is a raft-associated apical membrane protein with an unusual topology. *Traffic* **4,** 694–709
9. Hinz, A., Miguet, N., Natrajan, G., Usami, Y., Yamanaka, H., Renesto, P., Hartlieb, B., McCarthy, A. A., Simorre, J. P., Göttlinger, H., and Weissenhorn, W. (2010) Structural basis of HIV-1 tethering to membranes by the BST-2/tetherin ectodomain. *Cell Host Microbe* **7,** 314–323
10. Andrew, A. J., Miyagi, E., Kao, S., and Strebel, K. (2009) The formation of cysteine-linked dimers of BST-2/tetherin is important for inhibition of HIV-1 virus release but not for sensitivity to Vpu. *Retrovirology* **6,** 80
11. Perez-Caballero, D., Zang, T., Ebrahimi, A., McNatt, M. W., Gregory, D. A., Johnson, M. C., and Bieniasz, P. D. (2009) Tetherin inhibits HIV-1 release by directly tethering virions to cells. *Cell* **139,** 499–511
12. Venkatesh, S., and Bieniasz, P. D. (2013) Mechanism of HIV-1 virion entrapment by tetherin. *PLoS Pathog.* **9,** e1003483
13. Yang, H., Wang, J., Jia, X., McNatt, M. W., Zang, T., Pan, B., Meng, W., Wang, H. W., Bieniasz, P. D., and Xiong, Y. (2010) Structural insight into the mechanisms of enveloped virus tethering by tetherin. *Proc. Natl. Acad. Sci. U.S.A.* **107,** 18428–18432
14. Hammonds, J., Wang, J. J., Yi, H., and Spearman, P. (2010) Immunoelectron microscopic evidence for Tetherin/BST2 as the physical bridge between HIV-1 virions and the plasma membrane. *PLoS Pathog.* **6,** e1000749
15. Ono, A. (2010) Relationships between plasma membrane microdomains and HIV-1 assembly. *Biol. Cell* **102,** 335–350
16. Masuyama, N., Kuronita, T., Tanaka, R., Muto, T., Hirota, Y., Takigawa, A., Fujita, H., Aso, Y., Amano, J., and Tanaka, Y. (2009) HM1.24 is internalized from lipid rafts by clathrin-mediated endocytosis through interaction with α-adaptin. *J. Biol. Chem.* **284,** 15927–15941
17. Rollason, R., Korolchuk, V., Hamilton, C., Schu, P., and Banting, G. (2007) Clathrin-mediated endocytosis of a lipid-raft-associated protein is mediated through a dual tyrosine motif. *J. Cell Sci.* **120,** 3850–3858
18. Habermann, A., Krijnse-Locker, J., Oberwinkler, H., Eckhardt, M., Homann, S., Andrew, A., Strebel, K., and Kräusslich, H. G. (2010) CD317/tetherin is enriched in the HIV-1 envelope and downregulated from the plasma membrane upon virus infection. *J. Virol.* **84,** 4646–4658
19. Janvier, K., Pelchen-Matthews, A., Renaud, J. B., Caillet, M., Marsh, M., and Berlioz-Torrent, C. (2011) The ESCRT-0 component HRS is required for HIV-1 Vpu-mediated BST-2/tetherin down-regulation. *PLoS Pathog.* **7,** e1001265
20. Caillet, M., Janvier, K., Pelchen-Matthews, A., Delcroix-Genête, D., Camus, G., Marsh, M., and Berlioz-Torrent, C. (2011) Rab7A is required for efficient production of infectious HIV-1. *PLoS Pathog.* **7,** e1002347
21. Rollason, R., Korolchuk, V., Hamilton, C., Jepson, M., and Banting, G. (2009) A CD317/tetherin-RICH2 complex plays a critical role in the organization of the subapical actin cytoskeleton in polarized epithelial cells. *J. Cell Biol.* **184,** 721–736
22. Billcliff, P. G., Gorleku, O. A., Chamberlain, L. H., and Banting, G. (2013) The cytosolic N-terminus of CD317/tetherin is a membrane microdomain exclusion motif. *Biology Open* **2,** 1253–1263
23. Billcliff, P. G., Rollason, R., Prior, I., Owen, D. M., Gaus, K., and Banting, G. (2013) CD317/tetherin is an organiser of membrane microdomains. *J. Cell Sci.* **126,** 1553–1564
24. Iwabu, Y., Fujita, H., Kinomoto, M., Kaneko, K., Ishizaka, Y., Tanaka, Y., Sata, T., and Tokunaga, K. (2009) HIV-1 accessory protein Vpu internalizes cell-surface BST-2/tetherin through transmembrane interactions leading to lysosomes. *J. Biol. Chem.* **284,** 35060–35072
25. McNatt, M. W., Zang, T., Hatziioannou, T., Bartlett, M., Fofana, I. B., Johnson, W. E., Neil, S. J., and Bieniasz, P. D. (2009) Species-specific activity of HIV-1 Vpu and positive selection of tetherin transmembrane domain variants. *PLoS Pathog.* **5,** e1000300
26. Jia, X., Weber, E., Tokarev, A., Lewinski, M., Rizk, M., Suarez, M., Guatelli, J., and Xiong, Y. (2014) Structural basis of HIV-1 Vpu-mediated BST2 antagonism via hijacking of the clathrin adaptor protein complex 1. *eLife* **3,** e02362
27. Dubé, M., Paquay, C., Roy, B. B., Bego, M. G., Mercier, J., and Cohen, E. A. (2011) HIV-1 Vpu antagonizes BST-2 by interfering mainly with the trafficking of newly synthesized BST-2 to the cell surface. *Traffic* **12,** 1714–1729
28. Mitchell, R. S., Katsura, C., Skasko, M. A., Fitzpatrick, K., Lau, D., Ruiz, A., Stephens, E. B., Margottin-Goguet, F., Benarous, R., and Guatelli, J. C. (2009) Vpu antagonizes BST-2-mediated restriction of HIV-1 release via β-TrCP and endo-lysosomal trafficking. *PLoS Pathog.* **5,** e1000450
29. McNatt, M. W., Zang, T., and Bieniasz, P. D. (2013) Vpu binds directly to tetherin and displaces it from nascent virions. *PLoS Pathog.* **9,** e1003299
30. Lewinski, M. K., Jafari, M., Zhang, H., Opella, S. J., and Guatelli, J. (2015) Membrane anchoring by a C-terminal tryptophan enables HIV-1 Vpu to displace bone marrow stromal antigen 2 (BST2) from sites of viral assembly. *J. Biol. Chem.* **290,** 10919–10933
31. Andrew, A., and Strebel, K. (2011) The interferon-inducible host factor bone marrow stromal antigen 2/tetherin restricts virion release, but is it actually a viral restriction factor? *J. Interferon Cytokine Res.* **31,** 137–144
32. Malim, M. H., and Bieniasz, P. D. (2012) HIV Restriction factors and mechanisms of evasion. *Cold Spring Harb. Perspect. Med.* **2,** a006940
33. Harris, R. S., Hultquist, J. F., and Evans, D. T. (2012) The restriction factors of human immunodeficiency virus. *J. Biol. Chem.* **287,** 40875–40883
34. Kim, H., and McCulloch, C. A. (2011) Filamin A mediates interactions between cytoskeletal proteins that control cell adhesion. *FEBS Lett.* **585,** 18–22
35. Nakamura, F., Stossel, T. P., and Hartwig, J. H. (2011) The filamins: organizers of cell structure and function. *Cell Adh. Migr.* **5,** 160–169
36. Heuzé, M. L., Lamsoul, I., Baldassarre, M., Lad, Y., Lévêque, S., Razinia, Z., Moog-Lutz, C., Calderwood, D. A., and Lutz, P. G. (2008) ASB2 targets filamins A and B to proteasomal degradation. *Blood* **112,** 5130–5140
37. van der Flier, A., Kuikman, I., Kramer, D., Geerts, D., Kreft, M., Takafuta, T., Shapiro, S. S., and Sonnenberg, A. (2002) Different splice variants of filamin-B affect myogenesis, subcellular distribution, and determine binding to integrin β subunits. *J. Cell Biol.* **156,** 361–376
38. Lehmann, M., Rocha, S., Mangeat, B., Blanchet, F., Uji-I, H., Hofkens, J., and Piguet, V. (2011) Quantitative multicolor super-resolution microscopy reveals tetherin HIV-1 interaction. *PLoS Pathog.* **7,** e1002456
39. Luo, K., Liu, B., Xiao, Z., Yu, Y., Yu, X., Gorelick, R., and Yu, X. F. (2004) Amino-terminal region of the human immunodeficiency virus type 1 nucleocapsid is required for human APOBEC3G packaging. *J. Virol.* **78,** 11841–11852
40. Klimkait, T., Strebel, K., Hoggan, M. D., Martin, M. A., and Orenstein, J. M. (1990) The human immunodeficiency virus type 1-specific protein Vpu is required for efficient virus maturation and release. *J. Virol.* **64,** 621–629
41. Adachi, A., Gendelman, H. E., Koenig, S., Folks, T., Willey, R., Rabson, A., and Martin, M. A. (1986) Production of acquired immunodeficiency syn-

drome-associated retrovirus in human and nonhuman cells transfected with an infectious molecular clone. *J. Virol.* **59,** 284–291
42. Nguyen, K. L., llano, M., Akari, H., Miyagi, E., Poeschla, E. M., Strebel, K., and Bour, S. (2004) Codon optimization of the HIV-1 vpu and vif genes stabilizes their mRNA and allows for highly efficient Rev-independent expression. *Virology* **319,** 163–175
43. Woo, M. S., Ohta, Y., Rabinovitz, I., Stossel, T. P., and Blenis, J. (2004) Ribosomal S6 kinase (RSK) regulates phosphorylation of filamin A on an important regulatory site. *Mol. Cell. Biol.* **24,** 3025–3035
44. Cooper, J., Liu, L., Woodruff, E. A., Taylor, H. E., Goodwin, J. S., D'Aquila, R. T., Spearman, P., Hildreth, J. E., and Dong, X. (2011) Filamin A protein interacts with human immunodeficiency virus type 1 Gag protein and contributes to productive particle assembly. *J. Biol. Chem.* **286,** 28498–28510
45. Cunningham, C. C., Gorlin, J. B., Kwiatkowski, D. J., Hartwig, J. H., Janmey, P. A., Byers, H. R., and Stossel, T. P. (1992) Actin-binding protein requirement for cortical stability and efficient locomotion. *Science* **255,** 325–327
46. Takafuta, T., Wu, G., Murphy, G. F., and Shapiro, S. S. (1998) Human β-filamin is a new protein that interacts with the cytoplasmic tail of glycoprotein Ibα. *J. Biol. Chem.* **273,** 17531–17538
47. van der Flier, A., and Sonnenberg, A. (2001) Structural and functional aspects of filamins. *Biochim. Biophys. Acta* **1538,** 99–117
48. Kesner, B. A., Milgram, S. L., Temple, B. R., and Dokholyan, N. V. (2010) Isoform divergence of the filamin family of proteins. *Mol. Biol. Evol.* **27,** 283–295
49. Feng, S., Lu, X., and Kroll, M. H. (2005) Filamin A binding stabilizes nascent glycoprotein Ibα trafficking and thereby enhances its surface expression. *J. Biol. Chem.* **280,** 6709–6715
50. Fiori, J. L., Zhu, T. N., O'Connell, M. P., Hoek, K. S., Indig, F. E., Frank, B. P., Morris, C., Kole, S., Hasskamp, J., Elias, G., Weeraratna, A. T., and Bernier, M. (2009) Filamin A modulates kinase activation and intracellular trafficking of epidermal growth factor receptors in human melanoma cells. *Endocrinology* **150,** 2551–2560
51. Sverdlov, M., Shinin, V., Place, A. T., Castellon, M., and Minshall, R. D. (2009) Filamin A regulates caveolae internalization and trafficking in endothelial cells. *Mol. Biol. Cell* **20,** 4531–4540
52. Cho, E. Y., Cho, D. I., Park, J. H., Kurose, H., Caron, M. G., and Kim, K. M. (2007) Roles of protein kinase C and actin-binding protein 280 in the regulation of intracellular trafficking of dopamine D3 receptor. *Mol. Endocrinol.* **21,** 2242–2254
53. Yang, S. J., Lopez, L. A., Exline, C. M., Haworth, K. G., and Cannon, P. M. (2011) Lack of adaptation to human tetherin in HIV-1 group O and P. *Retrovirology* **8,** 78
54. Liu, G., Thomas, L., Warren, R. A., Enns, C. A., Cunningham, C. C., Hartwig, J. H., and Thomas, G. (1997) Cytoskeletal protein ABP-280 directs the intracellular trafficking of Furin and Modulates proprotein processing in the endocytic pathway. *J. Cell Biol.* **139,** 1719–1733
55. Noam, Y., Ehrengruber, M. U., Koh, A., Feyen, P., Manders, E. M., Abbott, G. W., Wadman, W. J., and Baram, T. Z. (2014) Filamin A promotes dynamin-dependent internalization of hyperpolarization-activated cyclic nucleotide-gated type 1 (HCN1) channels and restricts Ih in hippocampal neurons. *J. Biol. Chem.* **289,** 5889–5903
56. Rafizadeh, S., Zhang, Z., Woltz, R. L., Kim, H. J., Myers, R. E., Lu, L., Tuteja, D., Singapuri, A., Bigdeli, A. A., Harchache, S. B., Knowlton, A. A., Yarov-Yarovoy, V., Yamoah, E. N., and Chiamvimonvat, N. (2014) Functional interaction with filamin A and intracellular Ca^{2+} enhance the surface membrane expression of a small-conductance Ca^{2+}-activated K^+ (SK2) channel. *Proc. Natl. Acad. Sci. U.S.A.* **111,** 9989–9994
57. Nakamura, F., Osborn, T. M., Hartemink, C. A., Hartwig, J. H., and Stossel, T. P. (2007) Structural basis of filamin A functions. *J. Cell Biol.* **179,** 1011–1025
58. Stahlhut, M., and van Deurs, B. (2000) Identification of filamin as a novel ligand for caveolin-1: evidence for the organization of caveolin-1-associated membrane domains by the actin cytoskeleton. *Mol. Biol. Cell* **11,** 325–337
59. Muriel, O., Echarri, A., Hellriegel, C., Pavón, D. M., Beccari, L., and Del Pozo, M. A. (2011) Phosphorylated filamin A regulates actin-linked caveolae dynamics. *J. Cell Sci.* **124,** 2763–2776
60. Janvier, K., Roy, N., and Berlioz-Torrent, C. (2012) Role of the endosomal ESCRT machinery in HIV-1 Vpu-induced down-regulation of BST2/tetherin. *Curr. HIV Res.* **10,** 315–320
61. Arias, J. F., Iwabu, Y., and Tokunaga, K. (2012) Sites of action of HIV-1 Vpu in BST-2/tetherin downregulation. *Curr. HIV Res.* **10,** 283–291
62. Tokarev, A. A., Munguia, J., and Guatelli, J. C. (2011) Serine-threonine ubiquitination mediates downregulation of BST-2/tetherin and relief of restricted virion release by HIV-1 Vpu. *J. Virol.* **85,** 51–63
63. Pardieu, C., Vigan, R., Wilson, S. J., Calvi, A., Zang, T., Bieniasz, P., Kellam, P., Towers, G. J., and Neil, S. J. (2010) The RING-CH ligase K5 antagonizes restriction of KSHV and HIV-1 particle release by mediating ubiquitin-dependent endosomal degradation of tetherin. *PLoS Pathog.* **6,** e1000843
64. Agromayor, M., Soler, N., Caballe, A., Kueck, T., Freund, S. M., Allen, M. D., Bycroft, M., Perisic, O., Ye, Y., McDonald, B., Scheel, H., Hofmann, K., Neil, S. J., Martin-Serrano, J., and Williams, R. L. (2012) The UBAP1 subunit of ESCRT-I interacts with ubiquitin via a SOUBA domain. *Structure* **20,** 414–428
65. Stefani, F., Zhang, L., Taylor, S., Donovan, J., Rollinson, S., Doyotte, A., Brownhill, K., Bennion, J., Pickering-Brown, S., and Woodman, P. (2011) UBAP1 is a component of an endosome-specific ESCRT-I complex that is essential for MVB sorting. *Curr. Biol.* **21,** 1245–1250
66. Hayer, A., Stoeber, M., Ritz, D., Engel, S., Meyer, H. H., and Helenius, A. (2010) Caveolin-1 is ubiquitinated and targeted to intralumenal vesicles in endolysosomes for degradation. *J. Cell Biol.* **191,** 615–629
67. Skasko, M., Wang, Y., Tian, Y., Tokarev, A., Munguia, J., Ruiz, A., Stephens, E. B., Opella, S. J., and Guatelli, J. (2012) HIV-1 Vpu protein antagonizes innate restriction factor BST-2 via lipid-embedded helix-helix interactions. *J. Biol. Chem.* **287,** 58–67
68. Kobayashi, T., Ode, H., Yoshida, T., Sato, K., Gee, P., Yamamoto, S. P., Ebina, H., Strebel, K., Sato, H., and Koyanagi, Y. (2011) Identification of amino acids in the human tetherin transmembrane domain responsible for HIV-1 Vpu interaction and susceptibility. *J. Virol.* **85,** 932–945
69. Vigan, R., and Neil, S. J. (2010) Determinants of tetherin antagonism in the transmembrane domain of the human immunodeficiency virus type 1 Vpu protein. *J. Virol.* **84,** 12958–12970
70. Sauter, D. (2014) Counteraction of the multifunctional restriction factor tetherin. *Front. Microbiol.* **5,** 163
71. Roy, N., Pacini, G., Berlioz-Torrent, C., and Janvier, K. (2014) Mechanisms underlying HIV-1 Vpu-mediated viral egress. *Front. Microbiol.* **5,** 177
72. Strebel, K. (2014) HIV-1 Vpu: an ion channel in search of a job. *Biochim. Biophys. Acta* **1838,** 1074–1081
73. Douglas, J. L., Viswanathan, K., McCarroll, M. N., Gustin, J. K., Früh, K., and Moses, A. V. (2009) Vpu directs the degradation of the human immunodeficiency virus restriction factor BST-2/Tetherin via a βTrCP-dependent mechanism. *J. Virol.* **83,** 7931–7947
74. Mangeat, B., Gers-Huber, G., Lehmann, M., Zufferey, M., Luban, J., and Piguet, V. (2009) HIV-1 Vpu neutralizes the antiviral factor Tetherin/BST-2 by binding it and directing its β-TrCP2-dependent degradation. *PLoS Pathog.* **5,** e1000574
75. Dubé, M., Roy, B. B., Guiot-Guillain, P., Binette, J., Mercier, J., Chiasson, A., and Cohen, E. A. (2010) Antagonism of tetherin restriction of HIV-1 release by Vpu involves binding and sequestration of the restriction factor in a perinuclear compartment. *PLoS Pathog.* **6,** e1000856
76. Schmidt, S., Fritz, J. V., Bitzegeio, J., Fackler, O. T., and Keppler, O. T. (2011) HIV-1 Vpu blocks recycling and biosynthetic transport of the intrinsic immunity factor CD317/tetherin to overcome the virion release restriction. *MBio* **2,** e00036–00011